

Received January 1, 2021, accepted January 27, 2021, date of publication February 26, 2021, date of current version June 3, 2021.

Digital Object Identifier 10.1109/ACCESS.2021.3062278

# Magnetization Loss in HTS Coated Conductor Exposed to Harmonic External Magnetic Fields for Superconducting Rotating Machine Applications

MOHAMMAD YAZDANI-ASRAMI<sup>1</sup>, (Member, IEEE), WENJUAN SONG<sup>2</sup>, (Member, IEEE), MIN ZHANG<sup>1</sup>, (Member, IEEE), WEIJIA YUAN<sup>1</sup>, (Senior Member, IEEE), AND XIAOZE PEI<sup>2</sup>, (Member, IEEE)

<sup>1</sup>Department of Electronic and Electrical Engineering, University of Strathclyde, Glasgow G1 1XW, U.K.

<sup>2</sup>Department of Electronic & Electrical Engineering, University of Bath, Bath BA2 7AY, U.K.

Corresponding author: Mohammad Yazdani-Asrami (mohammad.yazdani-asrami@strath.ac.uk)

This work was supported in part by the U.K. Engineering and Physical Sciences Research Council (EPSRC) under Grant EP/S000720/1, and in part by the Innovate U.K. Project under Grant UKCG/11030.

**ABSTRACT** Previous studies on magnetization AC loss of high temperature superconducting (HTS) coated conductors (CCs) taken into account the ideally sinusoidal external magnetic field, or non-sinusoidal by considering only the harmonics in phase with the fundamental component. However, realistically magnetic field often contains harmonics with different phase angles and amplitudes. In this paper, magnetization AC loss in HTS CC was studied, considering the phase angle  $\varphi$  of each harmonic; assuming superconductor is subjected to external magnetic field which is distorted by the 3<sup>rd</sup> and the 5<sup>th</sup> harmonics. Phase angle of each harmonic was considered in the range of 0 to  $\pi$  and amplitude of fundamental magnetic field, was assumed as 10, 20, 50, and 100 mT. Different distortion level of magnetic field was considered too. It is concluded that phase angle of field harmonic has a significant effect on magnetization loss of HTS CCs.


**INDEX TERMS** External magnetic field, harmonic phase angle, HTS coated conductor, magnetization AC loss.

## I. INTRODUCTION

Large scale power applications of high temperature superconductors (HTS) have attracted tremendous attention in recent decades thanks to their advantages such as high current-carrying capacity, and low losses, for the cryoelectrification in both grid and specially in transportation systems, including rail, marine, and aviation applications [1]–[7]. HTS coated conductors (CCs) in these applications are mostly exposed to external magnetic field, which is ideally expected to be purely sinusoidal [7], [8]. Magnetic field is intermediary of the energy conversion in most of large-scale power applications such as superconducting rotating electric machines. The essence of magnetic field in a rotating electric machine could be non-sinusoidal, due to [9]–[12]: 1) coil/winding distribution in the machine stator, 2) manufacturing tolerances in the construction and assembly process, 3) occurrence of mechanical faults, such as bearing

wearing, or dynamic and static eccentricity faults. In such cases, the magnetic field would not be purely sinusoidal and thus, will contain harmonics. Such distorted magnetic fields cause extra losses in different parts of the machine, from core to HTS coils/windings [10]–[14]. It is vital to precisely estimate the magnetization AC loss in HTS CC under nonsinusoidal external magnetic field in order to develop reliable superconducting application, in particular, for sensitive applications such as electric aircrafts or fusion reactors [14].

In [10], authors studied the effect of harmonic amplitude as well as magnetic field dependency of critical current density on harmonic magnetization loss for ReBCO tapes. In [15], authors explored the AC loss in an HTS coil for wind turbine generators experimentally, under different DC field with AC ripples. In [16], [17], AC loss in HTS strip under nonsinusoidal current and magnetic field was formulated analytically, only considering harmonic amplitude. In [18], authors studied the total AC loss in a Bi-2223/Ag tape by considering a phase shift between sinusoidal magnetic field and sinusoidal transport current. In [19], [20], AC losses in

The associate editor coordinating the review of this manuscript and approving it for publication was Lei Chen .

a circular HTS double pancake coil under three different nonsinusoidal current/magnetic fields, including saw-tooth, triangle, and square waveforms, were measured and modelled considering the effect of amplitude, orientation angle, and frequency of applied waveforms.

There is a gap in addressing the dependence of magnetization loss in HTS CC on the phase angle of harmonics of external magnetic field in literature [10]–[21]. Our previous study observed a drastic transport AC loss variation when the current harmonic introduced at different phase angles [22]–[23].

In this work, we carried out comprehensive numerical calculations to investigate the magnetization loss in HTS CC subjected to distorted external magnetic field with the 3<sup>rd</sup> and the 5<sup>th</sup> harmonic orders at different phase angles ranging from 0 to  $2\pi$ . The amplitude of fundamental magnetic field varies from 10, 20, 50, and 100 mT. The effect of distortion level of different harmonic orders on magnetization loss in HTS CC was also discussed.

## II. MODELLING METHOD

Numerical calculations were implemented in COMSOL Multiphysics using 2D finite element (FE) approach, by means of  $H$  formulation method [24]–[29]. Two independent variables were implemented in the model,  $\mathbf{H} = [H_x, H_y]^T$ , where  $H_x$  and  $H_y$  are parallel and perpendicular magnetic fields, respectively.  $E$ - $J$  power law, as seen in (1) was used to characterize the nonlinear relation of local electric field  $E$  and local current density  $J$  in HTS CC [24], [25]:

$$E/J = (E_0/J_c(B)) (|J/J_c(B)|)^{n-1} \quad (1)$$

where  $B$  is magnetic field,  $E_0 = 1 \mu\text{V/cm}$ ,  $n$  is the constant derived from  $V$ - $I$  characteristic, and  $J_c(B)$  is the critical current density dependence on external magnetic field. Here, a modified Kim model was adopted, as expressed in (2).  $J_{c0}$  is the self-field critical current density. The  $k$ ,  $\alpha$ , and  $B_0$  are curve fitting parameters picked up from [30], [31].

$$J_c(B) = J_{c0} \left( 1 + \left( k^2 B_x^2 + B_y^2 \right) / B_0^2 \right)^{-\alpha} \quad (2)$$

The governing equation is as follows:

$$\partial(\mu_0 \mu_r \mathbf{H}) / \partial t + \nabla \times (\rho \nabla \times \mathbf{H}) = 0 \quad (3)$$

In the model, parallel magnetic field was set to 0,  $H_x = 0$ ; perpendicular magnetic field with harmonic component,  $H_y(t)$ , has been applied as formulated in (4),

$$H_y(t) = \frac{B_1}{\mu_0} \sin(2\pi ft) + \frac{B_1}{\mu_0} \text{THD}_k \sin(2\pi kft + \varphi_k) \quad (4)$$

In this model,  $f = 50$  Hz was considered.  $\text{THD}_k$  was defined to denote the distortion level of external magnetic field caused by each harmonic component,  $\text{THD}_k = B_{hk}/B_1$ , where  $k$  is the order of magnetic field harmonic,  $k = \{3, 5\}$ ; and  $\text{THD}_k = \{0.02, 0.05, 0.1, 0.15, \text{ and } 0.2\}$  were considered in this paper, i.e.  $\text{THD}_k \% = \{2, 5, 10, 15, \text{ and } 20\} \%$ .  $B_{hk}$  is amplitude of each harmonic magnetic field and  $B_1$  represents the amplitude of fundamental external magnetic field; here,

TABLE 1. Specifications of HTS coated conductor.

Parameter	Value
Manufacturer	SuperPower
Thickness of superconducting layer ( $t_{sc}$ ), $\mu\text{m}$	1
Width of tape ( $w_{\text{tape}}$ ), mm	4
Thickness of tape ( $t_{\text{tape}}$ ), mm	0.095
Critical current ( $J_{c0}$ ) @ 77K, A	86
$E$ - $J$ power law factor ( $n$ )	30
Characteristic electric field ( $E_0$ ) @ 77K, $\mu\text{V/cm}$	1
Stabilizer material	Copper
Substrate material	Hastelloy

$B_1 = \{10, 20, 50, \text{ and } 100\}$  mT. It is worthwhile to mention that the phase angle  $\varphi_k$  of each magnetic field harmonic varies from 0 to  $2\pi$  (i.e.,  $0^\circ$  to  $360^\circ$ ), here  $k = \{3, 5\}$ . The effect of phase angle of harmonic on magnetization AC losses was characterized by every 10 degrees, i.e.  $\varphi_k = \{0 : 10^\circ : 360^\circ\}$ .

## III. HARMONIC MAGNETIZATION AC LOSS: RESULTS AND DISCUSSIONS

A 4-mm wide SuperPower tape was chosen to calculate the magnetization loss under distorted external magnetic fields. The main specifications of this tape are tabulated in Table 1.

### A. EFFECT OF HARMONIC PHASE ANGLE ON MAGNETIZATION AC LOSSES

Fig. 1(a) and Fig. 1(b) illustrate the net external magnetic field per unit (P.U.) containing the 3<sup>rd</sup> and the 5<sup>th</sup> harmonics, respectively, at  $\varphi_k = \{0, 90^\circ, 180^\circ\}$ , compared with the pure sinusoidal magnetic field. In Fig. 1(a), the peak value of nonsinusoidal external magnetic field,  $A_{\text{nemf}}$ , has changed when  $\varphi_3$  varies, and it follows  $A_{\text{nemf}, \varphi_3=180} > A_{\text{nemf}, \varphi_3=90} > A_{\text{nemf}, \text{sine}} > A_{\text{nemf}, \varphi_3=0}$ . In Fig. 1(b), there exists  $A_{\text{nemf}, \varphi_5=0} > A_{\text{nemf}, \varphi_5=90} > A_{\text{nemf}, \text{sine}} > A_{\text{nemf}, \varphi_5=180}$ .

Fig. 2(a) and Fig. 2(b) show the magnetization AC loss in HTS CC subjected to the external magnetic field which is distorted by the 3<sup>rd</sup> and the 5<sup>th</sup> harmonic, respectively, at  $\text{THD} = 0.05$  and  $B_1 = \{10, 20, 50, 100\}$  mT, plotted versus phase angle of harmonic magnetic field  $\varphi$ . It has been observed in both Fig. 2(a)-(b) that, magnetization AC loss in HTS CC drastically increases with the increase of  $B_1$ , at a fixed THD value.

Figs. 3(a)-(d) report calculated magnetization AC losses in HTS CC subjected to nonsinusoidal external magnetic field with the 3<sup>rd</sup> and the 5<sup>th</sup> harmonics, respectively, at  $\text{THD}_k = 0.05$  for  $B_1 = \{10, 20, 50, \text{ and } 100 \text{ mT}\}$ , plotted against  $\varphi$  and compared with AC loss of sinusoidal external field,  $Q_{\text{sine}}$ . There are several phenomena observed from Fig. 3:

1) In Figs. 3(a)-(d), magnetization loss in HTS CC different  $\varphi_3$  follows:  $Q_{3\text{rd}, \varphi_3=180} > Q_{3\text{rd}, \varphi_3=90} > Q_{3\text{rd}, \text{sine}} > Q_{3\text{rd}, \varphi_3=0}$ , which aligns well with the peak value of nonsinusoidal external magnetic field,  $A_{\text{nemf}}$ , as shown in Fig. 1(a). Similarly, magnetization loss in HTS CC at different  $\varphi_5$  follows:  $Q_{5\text{th}, \varphi_5=0} > Q_{5\text{th}, \varphi_5=90} \geq Q_{5\text{th}, \text{sine}} > Q_{5\text{th}, \varphi_5=180}$ ,

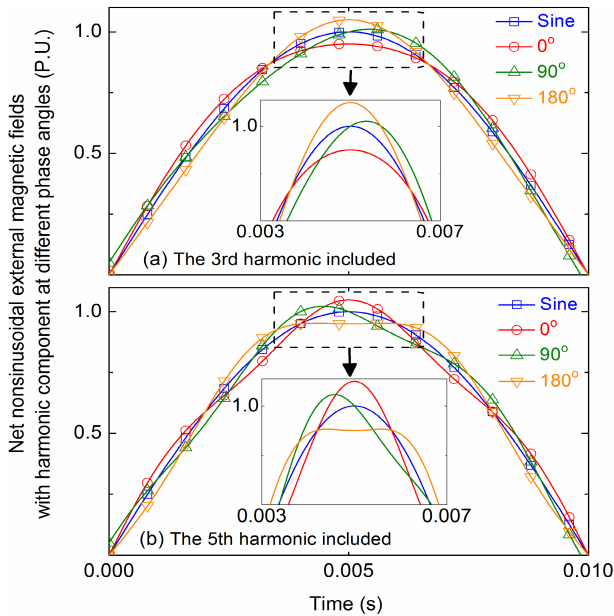


FIGURE 1. Net external magnetic field waveform distorted by harmonics at  $\varphi = \{0, 90^\circ, 180^\circ\}$ , plotted together with sinusoidal external magnetic field. (a) The 3<sup>rd</sup> harmonic included (b) The 5<sup>th</sup> harmonic included.

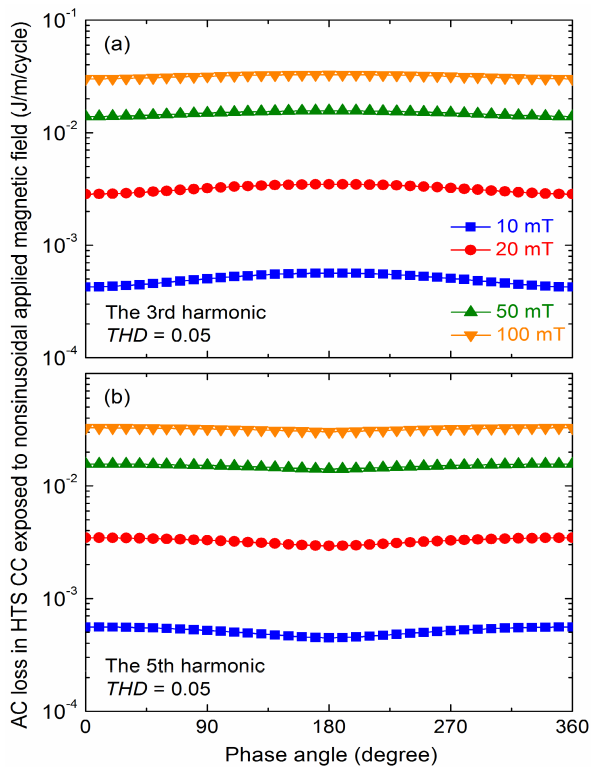


FIGURE 2. Magnetization AC losses in HTS CC subjected to nonsinusoidal external magnetic field with different fundamental magnetic field amplitude, plotted against phase angle of field harmonics: the 3<sup>rd</sup>, and the 5<sup>th</sup>, at  $THD_k = 0.05$ .

which agrees with the peak value of nonsinusoidal external magnetic field,  $A_{nemf}$ , shown in Fig. 1(b). This is to say, magnetization AC loss under nonsinusoidal external magnetic field is dependent on the peak magnitude of the nonsinusoidal

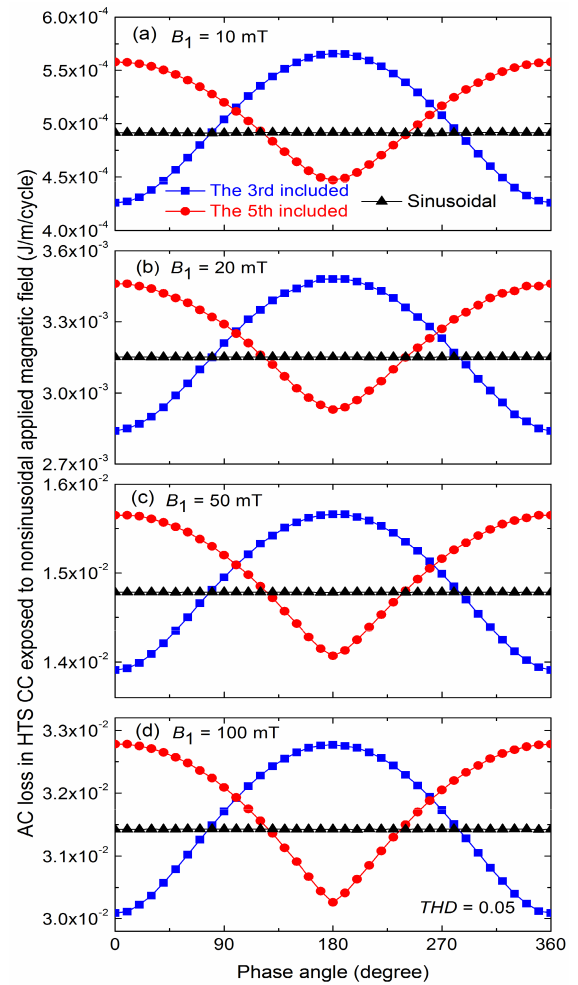
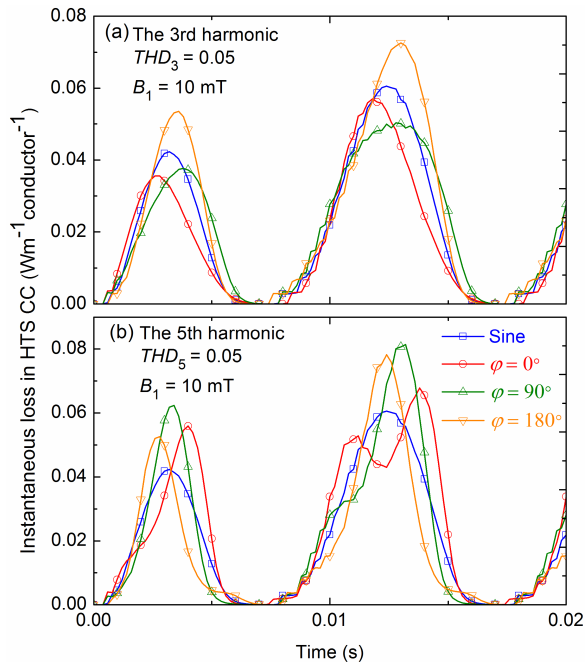


FIGURE 3. Magnetization AC losses in HTS CC subjected to sinusoidal external field and nonsinusoidal external magnetic field with the 3<sup>rd</sup>, and the 5<sup>th</sup> harmonics at  $THD_k = 0.05$  but different  $B_1$  values, plotted against phase angle.

external magnetic field,  $A_{nemf}$ . As the magnetization loss is a hysteresis type loss.

2) When an HTS CC is exposed to nonsinusoidal external magnetic field with the 3<sup>rd</sup> harmonic (or the 5<sup>th</sup> harmonic) at a given  $B_1$ , magnetization loss,  $Q_m$  changes at different  $\varphi$  value. When the 3<sup>rd</sup> harmonic was superimposed on the fundamental magnetic field,  $Q_m$  reaches the minimum at  $\varphi_3 = 0^\circ$  and it reaches the maximum at  $\varphi_3 = 180^\circ$ .  $Q_m$  is higher than  $Q_{sine}$  when  $80^\circ < \varphi_3 < 280^\circ$ , while it is lower than  $Q_{sine}$  when  $0^\circ < \varphi_3 < 80^\circ$ , and  $280^\circ < \varphi_3 < 360^\circ$ . This is due to the fact that phase angle of 3<sup>rd</sup> harmonics changes the peak of the net external magnetic field. However, when the 5<sup>th</sup> harmonic was superimposed on the fundamental magnetic field,  $Q_m$  reaches the minimum and maximum value at  $\varphi_5 = 180^\circ$  and  $\varphi_5 = 0^\circ$ , respectively.  $Q_m$  is higher than  $Q_{sine}$  when  $0^\circ < \varphi_5 < 120^\circ$ , and  $240^\circ < \varphi_5 < 360^\circ$ , while it is lower than  $Q_{sine}$  when  $120^\circ < \varphi_5 < 240^\circ$ .

3) It has been observed in Figs. 3(a)-(d) that,  $Q_m$  in HTS CC drastically increases with the increase of  $B_1$ , at a fixed



**FIGURE 4.** Instantaneous loss in HTS CC subjected to nonsinusoidal external magnetic field at  $B_1 = 10$  mT,  $THD_k = 0.05$ , and  $\varphi = \{0, 90^\circ, 180^\circ\}$ . (a) The 3<sup>rd</sup> harmonic included (b) The 5<sup>th</sup> harmonic included.

$THD = 0.05$ . When  $B_1$  increases from 10 to 100 mT,  $Q_m$  in HTS CC subjected to nonsinusoidal magnetic field with the 3<sup>rd</sup> harmonic increases by 110 times, and 85 times for the case of the 5<sup>th</sup> harmonic.

Fig. 4 and Fig. 5 plot and compare instantaneous losses in HTS CC exposed to the harmonics at lower and higher  $B_1$ , 10 mT and 100 mT, respectively, at  $\varphi_k = \{0^\circ, 90^\circ, 180^\circ\}$  and  $THD_k = 0.05$ . It is well known that AC loss is the integral of instantaneous loss over one period of applied external magnetic field. In Fig. 4, the maximum amplitude of instantaneous loss in case of the 5<sup>th</sup> harmonics are slightly higher than that of the 3<sup>rd</sup> harmonics. Two dominant peaks are observed in instantaneous loss profile resulted from distorted external magnetic field containing the 3<sup>rd</sup> harmonic, while there are three dominant peaks in the 5<sup>th</sup> harmonic case.

The maximum peak of instantaneous AC loss in case of the 3<sup>rd</sup> and the 5<sup>th</sup> harmonics belongs to  $\varphi_3 = 180^\circ$  and  $\varphi_5 = 90^\circ$ ; but the integration of instantaneous AC loss in one period is the highest at  $\varphi_3 = 180^\circ$  and  $\varphi_5 = 0^\circ$  for 3<sup>rd</sup> and 5<sup>th</sup> harmonics, respectively.

In Fig. 5, the amplitude of peaks of instantaneous loss has substantial improvement when  $B_1$  rises from 10 mT from 100 mT. The peaks are slightly higher for the 5<sup>th</sup> harmonics compared with the 3<sup>rd</sup> harmonic. At higher external magnetic field, the peak at  $\varphi = 0^\circ$  is always higher than others in both the 3<sup>rd</sup> and the 5<sup>th</sup> harmonic cases. But the integral of instantaneous loss (area under curve) reaches the maximum for the 3<sup>rd</sup> harmonic when  $\varphi = 180^\circ$ , and for 5<sup>th</sup> harmonic when  $\varphi = 0^\circ$ .

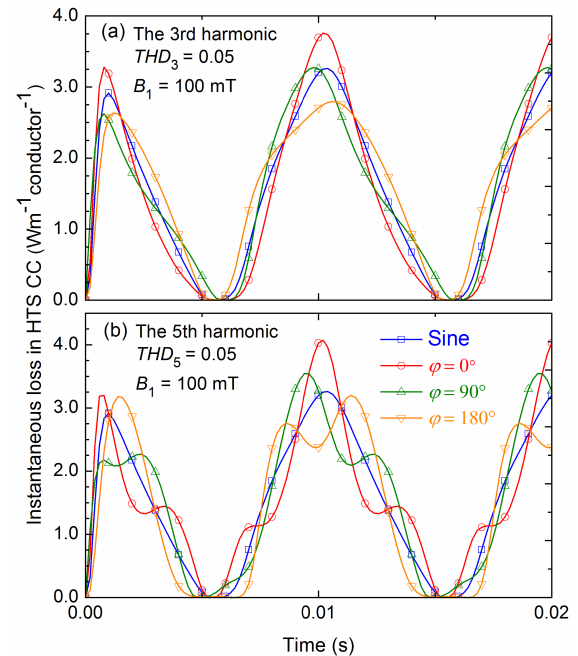


**FIGURE 5.** Instantaneous loss in HTS CC subjected to nonsinusoidal external magnetic field at  $B_1 = 100$  mT,  $THD_k = 0.05$ , and  $\varphi = \{0, 90^\circ, 180^\circ\}$ . (a) The 3<sup>rd</sup> harmonic included (b) The 5<sup>th</sup> harmonic included.

## B. EFFECT OF THD ON HARMONIC MAGNETIZATION AC LOSSES

Fig. 6(a) and Fig. 6(b) plot  $J/J_c$  distribution along the width of an HTS CC which is exposed to nonsinusoidal external magnetic field with the 3<sup>rd</sup> and 5<sup>th</sup> harmonics, respectively, at  $B_1 = 10$  mT and  $THD = \{0.05, 0.2\}$ . In Fig. 6(a), a bigger penetration depth was found at  $\varphi_3 = 180^\circ$  than  $\varphi_3 = 0^\circ$ , both at  $THD_3 = 0.05$  and 0.2. This is consistent with AC loss behavior shown in Fig. 3 that minimum and maximum  $Q_m$  occurs at  $\varphi_3 = 0^\circ$  and  $180^\circ$ . While at a given  $\varphi_3$  value, more  $J$  is penetrated in HTS CC at  $THD_3 = 0.2$ , compared to  $THD_3 = 0.05$ .

In Fig. 6(b), there is less  $J$  penetrated into the HTS CC at  $\varphi_5 = 180^\circ$  than  $\varphi_5 = 0^\circ$ , both at  $THD_5 = 0.05$  and 0.2. This is also in agreement with AC loss behavior shown in Fig. 3. At a given  $\varphi_5$  value, more  $J$  is penetrated in HTS CC at  $THD_5 = 0.2$ , compared to  $THD_5 = 0.05$ .

Fig. 7(a) and 7(b) report magnetization AC losses in HTS CC exposed to nonsinusoidal magnetic field with the 3<sup>rd</sup> and the 5<sup>th</sup> harmonics included, respectively, at fixed  $B_1 = 10$  mT but different  $THD_k$  values ranging from 0.02 to 0.2, plotted against phase angle of harmonic, and compared with  $Q_{sine}$ . Some phenomena/findings were found in Fig. 7:

1) AC loss in HTS CC exposed to nonsinusoidal magnetic field with the 3<sup>rd</sup> harmonic always reach the minimum at  $\varphi_3 = 0^\circ$  and the maximum at  $\varphi_3 = 180^\circ$ , at different THD values and  $B_1 = 10$  mT. AC loss in HTS CC exposed to nonsinusoidal magnetic field with the 5<sup>th</sup> harmonic always reach the minimum at  $\varphi_5 = 180^\circ$  and the maximum at  $\varphi_5 = 0^\circ$ , at different THD values and  $B_1 = 10$  mT.



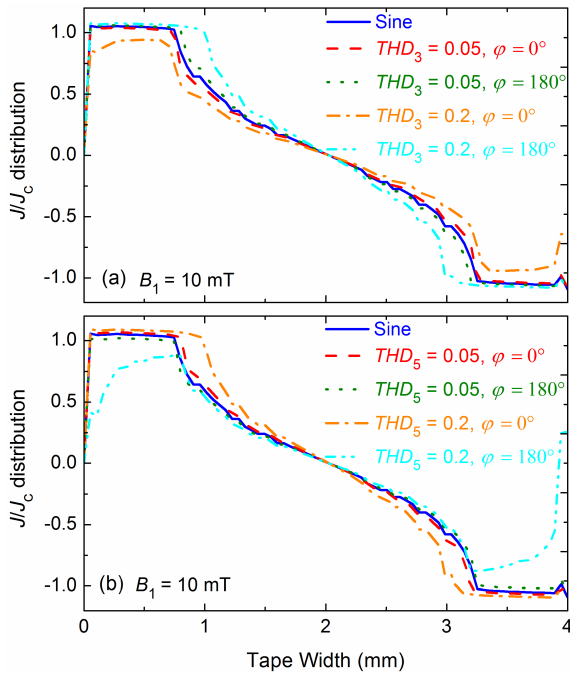


**FIGURE 6.**  $J/J_c$  distribution along the width of HTS CC exposed to nonsinusoidal external magnetic field at  $B_1 = 10$  mT and different THD level. (a) The 3<sup>rd</sup> harmonic included (b) The 5<sup>th</sup> harmonic included.

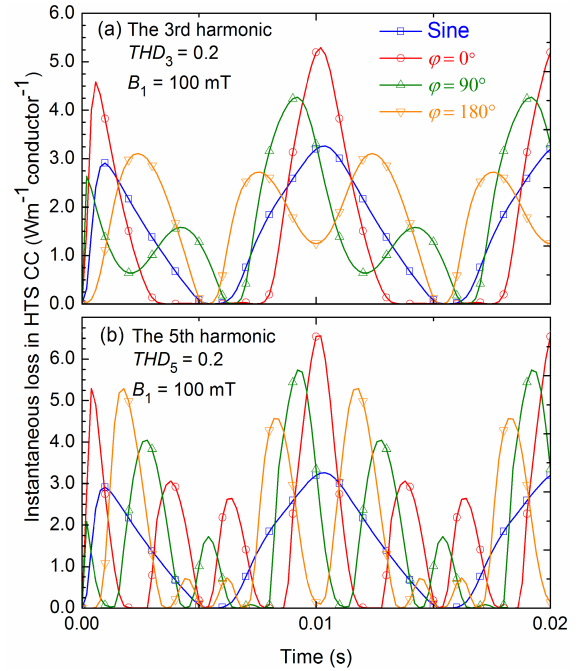


**FIGURE 8.** Instantaneous loss in HTS CC subjected to nonsinusoidal external magnetic field at  $B_1 = 100$  mT,  $THD_k = 0.2$ , and  $\varphi = \{0, 90^\circ, 180^\circ\}$ . (a) The 3<sup>rd</sup> harmonic included (b) The 5<sup>th</sup> harmonic included.

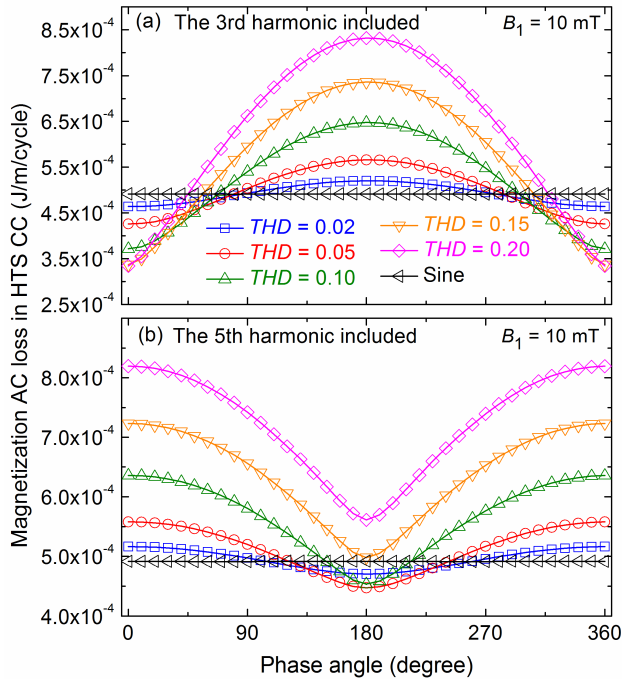


**FIGURE 7.** Magnetization AC losses in HTS CC subjected to nonsinusoidal external magnetic field with harmonics at  $B_1 = 10$  mT but different  $THD_k$  values ranging from 0.02 to 0.2, plotted against phase angle of magnetic field harmonics. (a) The 3<sup>rd</sup> harmonic included (b) The 5<sup>th</sup> harmonic included.

2)  $Q_{3rd,\varphi=0}$  and  $Q_{3rd,\varphi=180}$  are THD dependent, i.e.,  $Q_{3rd,\varphi=0}$  reduces with the increase of THD and  $Q_{3rd,\varphi=180}$  increases with the increase of THD, when THD varies from

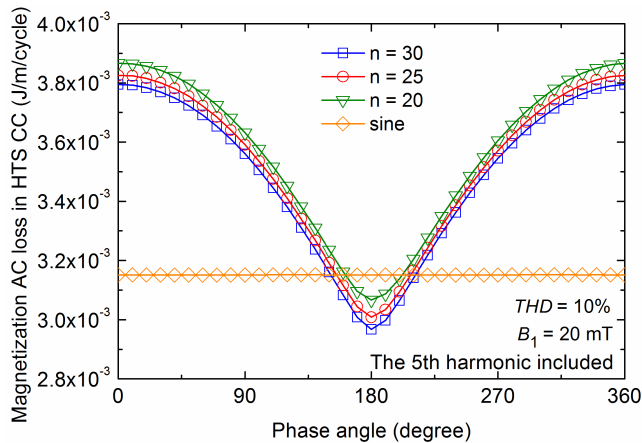
0.02 to 0.2. On the other hand,  $Q_{5th,\varphi=0}$  and  $Q_{5th,\varphi=180}$  are THD level dependent too, i.e.,  $Q_{5th,\varphi=0}$  increases with the increase of THD and  $Q_{5th,\varphi=180}$  reduces with the increase of THD, when THD varies from 0.02 to 0.2.

Fig. 8 reports the instantaneous AC loss of tape exposed to external magnetic field with the 3<sup>rd</sup> and the 5<sup>th</sup> harmonics at THD = 0.2 and  $B_1 = 100$  mT. The amplitude of peaks of instantaneous AC loss have been increased as compared to those in Fig. 4 when THD = 0.05 and  $B_1 = 100$  mT. However, the number of peaks in instantaneous loss distorted by the 5<sup>th</sup> harmonic is more obvious in THD = 0.2, as compared with THD = 0.05. Another interesting observation is that the number of peaks in THD<sub>5</sub> = 0.2 is higher than THD<sub>5</sub> = 0.05. It is because of higher fluctuation and distortion caused by the 5<sup>th</sup> harmonics.

**C. EFFECT OF n-VALUE AND B-DEPENDENCY OF CRITICAL CURRENT DENSITY ON HARMONIC MAGNETIZATION AC LOSSES**

As shown in Fig. 9, calculated magnetization losses of a single coated conductor get slightly increased around 2.1% when n-value decreases from 30 to 20, at THD<sub>5</sub> = 10%,  $B_1 = 20$  mT, and any phase angle. This is due to the fact that with a larger n-value, the E-J curve get steeper, approaching to critical state model. Actually, n-value, as a good indicator of the E-I resistive transition, shows that a larger n-value indicates the improvement of  $I_c$  of the superconductor, which leads to slightly lower AC losses [32].

In order to demonstrate the effect  $J_c(B)$  dependence on the nonsinusoidal AC losses, we carried out another calculation



**FIGURE 9.** Magnetization loss of superconductor when exposed to external magnetic field at  $B_1 = 20$  mT,  $THD_5 = 10\%$ , and varying  $n$  values.

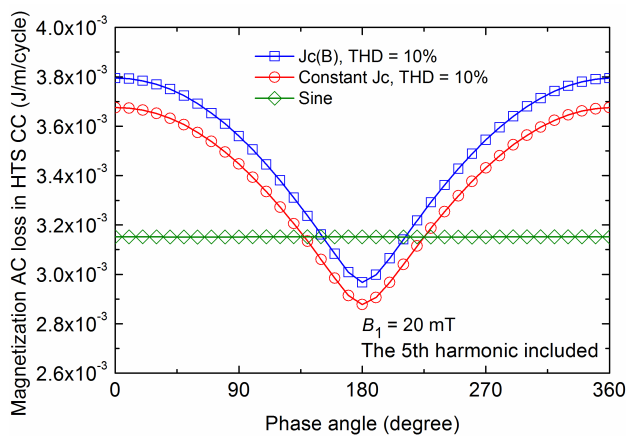


**FIGURE 10.** Magnetization loss of superconductor when exposed to external magnetic field at  $B_1 = 20$  mT,  $5rd$ ,  $THD = 10\%$ .

with constant  $J_c = J_{c0}$ , the self-field critical current density. The case study was done at  $B_1 = 20$  mT,  $THD_5 = 10\%$ . In Fig. 10, magnetization loss of a single coated conductor calculated by considering  $J_c(B)$  is always larger than that calculated by considering constant  $J_c$ , at  $B_1 = 20$  mT,  $THD_5 = 10\%$  and any phase angle. It is roughly estimated that the effective penetration field of the superconductor at self-field 77 K is 21.2 mT. When the  $J_c(B)$  effect is considered,  $J_c$  under external magnetic field will be degraded and thus, the penetration field will decrease, accordingly. In this case study, we chose 20 mT as the external magnetic field, which is smaller than the penetration field calculated by self-field  $J_c$  [33]. Therefore, when constant  $J_c$  is considered in the calculation, magnetization loss would be underestimated.

#### IV. CONCLUSION

In this paper, we carried out a series of numerical calculations to study the nonsinusoidal magnetization loss in HTS CC exposed to external magnetic field polluted with the 3<sup>rd</sup> and the 5<sup>th</sup> harmonic components, at various harmonic phase

angles  $\varphi$  ranging from  $0^\circ$  to  $360^\circ$  and different amplitudes of fundamental magnetic field  $B_1$ , and harmonic distortion level, denoted by THD, was chosen to be 0 to 0.2.

Magnetization loss in HTS CC under nonsinusoidal magnetic field with the 3<sup>rd</sup> harmonic meets the minimum and maximum at  $\varphi_3 = 0^\circ$  and  $\varphi_3 = 180^\circ$ , respectively, at a fixed  $B_1$  and THD values. On the contrary, magnetization loss in HTS CC under nonsinusoidal magnetic field with the 5<sup>th</sup> harmonic reaches the minimum and maximum at  $\varphi_5 = 180^\circ$  and  $\varphi_5 = 0^\circ$ , respectively. This is due to the compensation effect of magnetic field waveforms and the maximum peak of resultant nonsinusoidal magnetic field waveforms roughly dominates the AC loss.

Magnetization loss in HTS CC under external magnetic field with the 3<sup>rd</sup> or the 5<sup>th</sup> harmonic drastically increases with the increase of  $B_1$ , at a fixed THD in the range of 0 to 0.2 and a fixed phase angle in the range of  $0^\circ$  to  $360^\circ$ , due to deeper magnetic field penetration in HTS CC.

At a fixed  $B_1$  and phase angle, magnetization loss in HTS CC under external magnetic field with the 3<sup>rd</sup> or the 5<sup>th</sup> harmonic increases proportionally with the increase of THD.

#### REFERENCES

- [1] K. S. Haran, S. Kalsi, T. Arndt, H. Karmaker, R. Badcock, B. Buckley, T. Haugan, M. Izumi, D. Loder, J. W. Bray, P. Masson, and E. W. Stautner, "High power density superconducting rotating machines—Development status and technology roadmap," *Superconductor Sci. Technol.*, vol. 30, no. 12, 2017, Art. no. 123002.
- [2] M. Yazdani-Asrami, M. Zhang, and W. Yuan, "Challenges for developing high temperature superconducting ring magnets for rotating electric machine applications in future electric aircrafts," *J. Magn. Magn. Mater.*, vol. 522, Mar. 2021, Art. no. 167543.
- [3] Y. Wang, C. Wan Kan, and J. Schwartz, "Self-protection mechanisms in no-insulation (RE)  $Ba_2Cu_3O_x$  high temperature superconductor pancake coils," *Superconductor Sci. Technol.*, vol. 29, no. 4, Apr. 2016, Art. no. 045007.
- [4] W. Song, Z. Jiang, M. Staines, R. A. Badcock, S. C. Wimbush, J. Fang, and J. Zhang, "Design of a single-phase 6.5 MVA/25 kV superconducting traction transformer for the chinese fuxing high-speed train," *Int. J. Electr. Power Energy Syst.*, vol. 119, Jul. 2020, Art. no. 105956.
- [5] B. Liu, S. Wang, B. Zhao, X. Wang, and J. Fang, "Research on AC losses of racetrack superconducting coils applied to high-temperature superconducting motors," *Superconductor Sci. Technol.*, vol. 32, no. 1, 2019, Art. no. 115010.
- [6] B. Liu, R. Badcock, H. Shu, L. Tan, and J. Fang, "Electromagnetic characteristic analysis and optimization design of a novel HTS coreless induction motor for high-speed operation," *IEEE Trans. Appl. Supercond.*, vol. 28, no. 4, pp. 1–5, Jun. 2018.
- [7] R. M. Scanlan, A. P. Malozemoff, and D. C. Larbalestier, "Superconducting materials for large scale applications," *Proc. IEEE*, vol. 92, no. 10, pp. 1639–1654, Oct. 2004.
- [8] W. Zhou, Z. Jiang, M. Staines, W. Song, C. W. Bumby, R. A. Badcock, N. J. Long, and J. Fang, "Magnetization loss in REBCO roebel cables with varying strand numbers," *IEEE Trans. Appl. Supercond.*, vol. 28, no. 3, pp. 1–5, Apr. 2018.
- [9] M. Yazdani-Asrami, M. Mirzaie, and A. Akmal, "No-load loss calculation of distribution transformers supplied by nonsinusoidal voltage using three-dimensional finite element analysis," *Energy*, vol. 50, pp. 205–219, Feb. 2013.
- [10] M. Yazdani-Asrami, S. A. Gholamian, S. M. Mirimani, and J. Adabi, "Calculation of AC magnetizing loss of REBCO superconducting tapes subjected to applied distorted magnetic fields," *J. Supercond. Novel Magn.*, vol. 31, no. 12, pp. 3875–3888, Dec. 2018.

- [11] R. Kulkarni, K. Prasad, T. Tjing Lie, R. A. Badcock, C. W. Bumby, and H. J. Sung, "Design improvisation for reduced harmonic distortion in a flux pump-integrated HTS generator," *Energies*, vol. 10, no. 9, p. 1344, 2017.
- [12] G. J. Wakileh, "Harmonics in rotating machines," *Electr. Power Syst. Res.*, vol. 66, no. 1, pp. 31–37, Jul. 2003.
- [13] B. Douine, J. Leveque, and A. Rezzoug, "AC loss measurements of a high critical temperature superconductor transporting sinusoidal or non-sinusoidal current," *IEEE Trans. Appl. Supercond.*, vol. 10, no. 1, pp. 1489–1492, Mar. 2000.
- [14] F. Grilli, E. Pardo, A. Stenvall, D. N. Nguyen, W. Yuan, and F. Gomory, "Computation of losses in HTS under the action of varying magnetic fields and currents," *IEEE Trans. Appl. Supercond.*, vol. 24, no. 1, Feb. 2014, Art. no. 8200433.
- [15] M. Chudy, Y. Chen, M. Zhang, M. Baghdadi, J. Lalk, T. Pretorius, and T. Coombs, "Power losses of 2G HTS coils measured in external magnetic DC and ripple fields," *IEEE Trans. Appl. Supercond.*, vol. 24, no. 1, Feb. 2014, Art. no. 8200606.
- [16] V. Sokolovsky, V. Meerovich, M. Spektor, G. A. Levin, and I. Vajda, "Losses in superconductors under non-sinusoidal currents and magnetic fields," *IEEE Trans. Appl. Supercond.*, vol. 19, no. 3, pp. 3344–3347, Jun. 2009.
- [17] G. Furman, M. Spektor, V. Meerovich, and V. Sokolovsky, "Losses in coated conductors under nonsinusoidal currents and magnetic fields," *J. Supercond. Novel Magn.*, vol. 24, nos. 1–2, pp. 1045–1051, Jan. 2011.
- [18] M. Vojenčiak, J. Šouc, J. M. Ceballos, F. Gömöry, B. Klinčok, E. Pardo, and F. Grilli, "Study of AC loss in bi-2223/Ag tape under the simultaneous action of AC transport current and AC magnetic field shifted in phase," *Superconductor Sci. Technol.*, vol. 19, no. 4, pp. 397–404, Apr. 2006.
- [19] B. Shen, C. Li, J. Geng, X. Zhang, J. Gawith, J. Ma, Y. Liu, F. Grilli, and T. A. Coombs, "Power dissipation in HTS coated conductor coils under the simultaneous action of AC and DC currents and fields," *Superconductor Sci. Technol.*, vol. 31, no. 7, pp. 1–12, 2018.
- [20] B. Shen, C. Li, J. Geng, Q. Dong, J. Ma, J. Gawith, K. Zhang, Z. Li, J. Chen, W. Zhou, X. Li, J. Sheng, Z. Li, Z. Huang, J. Yang, and T. A. Coombs, "Power dissipation in the HTS coated conductor tapes and coils under the action of different oscillating currents and fields," *IEEE Trans. Appl. Supercond.*, vol. 29, no. 5, pp. 1–5, Aug. 2019.
- [21] M. Yazdani-Asrami, S. Asghar Gholamian, S. M. Mirimani, and J. Adabi, "Influence of field-dependent critical current on harmonic AC loss analysis in HTS coils for superconducting transformers supplying non-linear loads," *Cryogenics*, vol. 113, Jan. 2021, Art. no. 103234.
- [22] M. Yazdani-Asrami, W. Song, M. Zhang, W. Yuan, and X. Pei, "AC transport loss in superconductors carrying harmonic current with different phase angles for large-scale power components," *IEEE Trans. Appl. Supercond.*, vol. 31, no. 1, pp. 1–5, Jan. 2021.
- [23] M. Yazdani-Asrami, M. Taghipour-Gorjikaie, W. Song, M. Zhang, and W. Yuan, "Prediction of nonsinusoidal AC loss of superconducting tapes using artificial intelligence-based models," *IEEE Access*, vol. 8, pp. 207287–207297, 2020.
- [24] Z. Hong, A. M. Campbell, and T. A. Coombs, "Numerical solution of critical state in superconductivity by finite element software," *Superconductor Sci. Technol.*, vol. 19, no. 12, pp. 1246–1252, Dec. 2006.
- [25] R. Brambilla, F. Grilli, and L. Martini, "Development of an edge-element model for AC loss computation of high-temperature superconductors," *Superconductor Sci. Technol.*, vol. 20, no. 1, pp. 16–24, Jan. 2007.
- [26] V. M. Rodriguez-Zermeño, N. Mijatovic, C. Traeholt, T. Zirngibl, E. Seiler, A. B. Abrahamson, N. F. Pedersen, and M. P. Sorensen, "Towards faster FEM simulation of thin film superconductors: A multiscale approach," *IEEE Trans. Appl. Supercond.*, vol. 21, no. 3, pp. 3273–3276, Jun. 2011.
- [27] W. Song, Z. Jiang, X. Zhang, M. Staines, R. A. Badcock, J. Fang, Y. Sogabe, and N. Amemiya, "AC loss simulation in a HTS 3-Phase 1 MVA transformer using h formulation," *Cryogenics*, vol. 94, pp. 14–21, Sep. 2018.
- [28] M. Yazdani-Asrami, S. A. Gholamian, S. M. Mirimani, and J. Adabi, "Investigation on effect of magnetic field dependency coefficient of critical current density on the AC magnetizing loss in HTS tapes exposed to external field," *J. Supercond. Novel Magn.*, vol. 31, no. 12, pp. 3899–3910, Dec. 2018.
- [29] S. Li, D. X. Chen, and J. Fang, "Transport AC losses of a second-generation HTS tape with a ferromagnetic substrate and conducting stabilizer," *Superconductor Sci. Technol.*, vol. 28, no. 12, 2015, Art. no. 125011.
- [30] W. Song, J. Fang, and Z. Jiang, "Numerical AC loss analysis in HTS stack carrying nonsinusoidal transport current," *IEEE Trans. Appl. Supercond.*, vol. 29, no. 2, pp. 1–5, Mar. 2019.
- [31] M. Yazdani-Asrami, W. Song, X. Pei, M. Zhang, and W. Yuan, "AC loss characterization of HTS pancake and solenoid coils carrying nonsinusoidal currents," *IEEE Trans. Appl. Supercond.*, vol. 30, no. 5, pp. 1–9, Aug. 2020.
- [32] S. Li and D. X. Chen, "Scaling law for voltage-current curve of a superconductor tape with a power-law dependence of electric field on a magnetic-field-dependent sheet current density," *Phys. C, Supercond. Appl.*, vol. 538, pp. 32–39, Jul. 2017.
- [33] Y. Liu, Z. Jiang, Q. Li, C. W. Bumby, R. A. Badcock, and J. Fang, "Dynamic resistance measurement in a four-tape YBCO stack with various applied field orientation," *IEEE Trans. Appl. Supercond.*, vol. 29, no. 5, pp. 1–7, Aug. 2019.



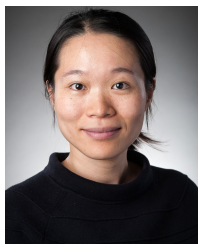
**MOHAMMAD YAZDANI-ASRAMI** (Member, IEEE) received the Ph.D. degree in electrical power engineering, in 2018.

In 2015, he was a Visiting Research Assistant on the Superconducting Machine Project with the Superconductivity Division of ENEA, Frascati, Italy. From 2016 to 2017, he worked as a Research Assistant on a project for design development and fabrication of a fault tolerant superconducting transformer at the Robinson Research Institute, Victoria University of Wellington, New Zealand. He also worked as a Project Engineer for testing electric machine and components with the University of Warwick, U.K. He is currently a Postdoctoral Research Associate with the Department of Electronic and Electrical Engineering, University of Strathclyde, Glasgow, U.K. His research interests include applied superconductivity for large-scale power applications, cryo-electrification for modern transportation systems, material characterization and AC loss calculation and measurement for HTS and MgB<sub>2</sub> tapes and wires, and design development of superconducting rotating machine, transformers, fault current limiters, and cables.



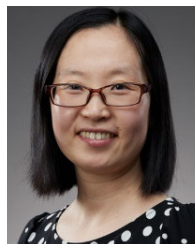
**WENJUAN SONG** (Member, IEEE) received the M.Eng. and Ph.D. degrees in electrical engineering from Beijing Jiaotong University (BJTU), China, in 2015 and 2019, respectively.

From 2016 to 2018, she was a Visiting Research Assistant with the Robinson Research Institute, Victoria University of Wellington, New Zealand. Since 2019, she has been a Postdoctoral Research Associate with the Department of Electronic & Electrical Engineering, University of Bath. Her research interests include electromagnetic analysis for superconducting power applications, AC loss calculation and measurement of superconductors, and design and development of superconducting fault current limiters and transformers.



**MIN ZHANG** (Member, IEEE) received the bachelor's and master's degrees from Tsinghua University, both in electrical engineering, and the Ph.D. degree in engineering from the University of Cambridge. She spent a year as a Junior Research Fellow with the Newnham College, Cambridge, and then joined the University of Bath, as a Lecturer. In 2018, she joined the University of Strathclyde, as a Reader, and is currently a Research Fellow with the Royal Academy of Engineering.

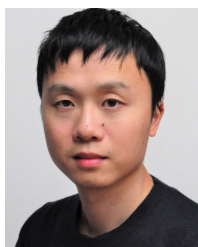
Her research interests include the application of high temperature superconductors in power system transmission, renewable generation, and electric transportation.



**XIAOZE PEI** (Member, IEEE) received the B.Eng. and M.Eng. degrees from Beijing Jiaotong University, Beijing, China, in 2006 and 2008, respectively, and the Ph.D. degree from The University of Manchester, Manchester, U.K., in 2012.

She was a Research Associate with The University of Manchester. In 2017, she joined the University of Bath, as a Lecturer. She has extensive research experience in designing and building of superconducting fault current limiters and fast operating vacuum circuit breakers. Her research interests include electrical power applications of superconductivity and hybrid DC circuit breaker.

• • •



**WEIJIA YUAN** (Senior Member, IEEE) received the bachelor's degree from Tsinghua University, in 2006, and the Ph.D. degree from the University of Cambridge, in 2010.

He then became a Research Associate with the Department of Engineering, University of Cambridge, and a Junior Research Fellow with the Wolfson College, University of Cambridge, from 2010 to 2011. In 2011, he joined the University of Bath, as a Lecturer/an Assistant Professor, where he was later promoted to a Reader/an Associate Professor, in 2016. In 2018, he joined the University of Strathclyde, as a Professor. He is currently leading a Research Team in the area applied superconductivity, including energy storage, fault current limiters, and machines and power transmission lines. He has been working closely with industry partners on all electric propulsion for future electric aircraft, and designing a fully superconducting system for aerospace application. His work also involves renewable energy integration and power system stability using energy storage systems.